PCCP



View Article Online PAPER



Cite this: Phys. Chem. Chem. Phys., 2017, 19, 24197

Received 6th May 2017, Accepted 18th July 2017

DOI: 10.1039/c7cp02994b

rsc.li/pccp

Electron ionization of helium droplets containing C₆₀ and alcohol clusters

M. Goulart, pab F. Zappa, bb A. M. Ellis, b*c P. Bartl, S. Ralser and P. Scheier*

We report a mass spectrometric investigation of $(C_{60})_n$ clusters mixed with either methanol or ethanol clusters inside helium nanodroplets. The abundance of ion products produced by electron ionization shows marked differences compared with pure methanol/ethanol clusters without C₆₀ [M. Goulart, P. Bartl, A. Mauracher, F. Zappa, A. M. Ellis and P. Scheier, Phys. Chem. Chem. Phys., 2013, 15, 3577], where clusters containing in excess of a hundred alcohol monomers were observed. In contrast, under identical conditions concerning He droplet size and alcohol pickup pressure, only a small number of alcohol molecules become attached to the fullerene ions. Our results suggest that each fullerene cluster acts as a charge sink, which hampers alcohol cluster formation, as well as intra-cluster ion-molecule reactions. The appearance of specific 'magic number' peaks suggests an enhanced probability for the attachment of small alcohol rings to $(C_{60})_n^+$ clusters.

1 Introduction

The diffuse interstellar bands (DIBs) are absorption bands in the visible and near-infrared that originate from molecules absorbing in the interstellar medium (ISM). 1,2 The identification of the carriers of these bands has proven to be a long-standing challenge and while various classes of molecules, such as polycyclic aromatic hydrocarbons,³ seem to possess some of the absorption characteristics, definitive assignments of specific bands have proved elusive. A breakthrough was made recently with the firm identification of C_{60}^{+} as the carrier of two DIBs in the near-infrared.⁴⁻⁷ The temperatures in cold molecular clouds and in the ISM can vary between 10 and 100 K. At such low temperatures weakly bound clusters and complexes may be longlived and therefore one must consider the possibility of C_{60} combining with other species in the ISM, since such complexes might be carriers of other DIBs.

Methanol is one of the most abundant organic molecules in the interstellar medium,8 with relative abundances, with respect to H₂, ranging from 10⁻⁶ in hot cores near high-mass protostars to 10^{-9} in cold, dark interstellar clouds. 9,10 Furthermore, it is generally agreed that the synthesis of this molecule can occur in the gas phase, 11,12 as well as from CO hydrogenation on icy surfaces of dust particles. 13,14 The latter mechanism is considered to be responsible for most of the methanol in the ISM. Given the abundance of methanol in the ISM, it is interesting to explore how this molecule can interact with C₆₀+, which has well known effects on the ionization processes of other species, notably cesium. 15,16 However, this poses a challenge, since one must find a way to combine ionized C₆₀ and methanol molecules at low temperature. Here we approach this problem by trapping the neutral molecules in liquid helium nanodroplets and then ionizing the system using electron ionization. Such an approach has been used previously for C₆₀ in combination with other small molecules, such as hydrogen, 17 water, 18,19 ammonia 20 and carbon dioxide.21

The electron ionization of pure methanol clusters in helium nanodroplets has been reported previously. 22,23 In the most recent study cluster ions containing up to 100 methanol monomers were observed.²³ The primary products were protonated methanol clusters ions, [(CH₃OH)_mH⁺], which matches earlier gas phase work.24-26 However, intra-cluster reactions were also induced by the ionization process, leading to the production of water molecules within the clusters. The observation of particularly stable ions in the mass spectra pointed towards hydrogenbonded structures consisting of five-membered rings.²³

In the current study we investigate how the ion chemistry of clusters of two small alcohols, methanol and ethanol, is affected by the presence of C₆₀. As we will see, the ion chemistry is very different from that of pure alcohol clusters. Although the alcohols do not wet the fullerene, 27 the latter nevertheless has a major impact on the chemistry of the former, suppressing prominent reaction channels seen for the pure alcohols. In addition, we see particular combinations of the alcohol clusters with clearly enhanced stabilities, so-called magic numbers, and report on those here.

^a Institut für Ionenphysik und Angewandte Physik, Innsbruck, A-6020, Austria. E-mail: paul.scheier@uibk.ac.at

^b Departamento de Física, UFJF, Juiz de Fora, MG, 36036-900, Brazil

^c Department of Chemistry, University of Leicester, UK. E-mail: andrew.ellis@le.ac.uk

2 Experimental

Paper

The apparatus used for these experiments is the same as in the previous investigation of pure alcohols.²³ Helium nanodroplets were produced by expanding ultra-pure helium (99.9999%) through a 5 µm aperture into a vacuum. In order to make the droplets the nozzle needs to be cooled to a low temperature, which was achieved by connection to a closed-cycle cryostat (Sumitomo RDK-415 F50H). For the present work, the helium stagnation pressure was 20 MPa and the nozzle temperature was 9 K, resulting in droplets containing $\sim 10^6$ helium atoms, on average. ²⁸ After formation the droplets passed through a skimmer with a 0.8 mm diameter aperture and entered two differentially-pumped vacuum chambers sequentially, where dopants were added. One chamber contained C₆₀ (SES research, 99.95%) vapor from a resistively heated crucible, while in the other alcohol vapor was added (methanol or ethanol, both from Sigma-Aldrich (99.8%)). In the present case the alcohol was introduced before the fullerenes, although the sequence of the pickup of the two dopants did not affect the results. Once inside a nanodroplet the dopants move in planar orbits below the Landau velocity and eventually find each other.29

The doped droplets then underwent ionization by a Nier type ion source at 70 eV electron energy. The ionization process starts when an electron produces a He $^+$ ion in the droplet. This positively charged hole is mobile and so can migrate from atom to atom *via* resonant hole hopping. The charged hole can encounter either the dopant molecule(s) and transfer the charge or it will localize and form a He $_n$ ⁺ structure. 30,31 Ions that escape from the droplet into the gas phase are accelerated up to an energy of 40 eV in an ion guide and then pass into the entrance of a commercial reflectron time-of-flight mass spectrometer (Tofwerk HTOF) with a mass resolution $m/\Delta m \sim 5000$ (FWHM).

3 Results

Methanol + C₆₀

Fig. 1(a) shows a mass spectrum obtained after electron ionization of helium droplets doped with C_{60} and methanol. The coarse structure in this overview mass spectrum is dominated by strong peaks originating from $(C_{60})_n^+$ cluster ions, with n up to 18 being easily seen in this particular spectrum. The finer details of the mass spectrum arise mainly from the addition of methanol molecules. Also present are He_n^+ cluster ions, which give rise to the dense signal at low masses. Due to the statistics of the pickup process, large fullerene clusters originate from large helium droplets. Consequently, the number of alcohol molecules being picked up will also be larger in these droplets than in smaller ones. The mass spectrum in Fig. 1(a) somewhat reflects this but the number of attached methanol molecules does not increase in strict accordance with the number of fullerene monomers.

Fig. 1(b) provides an expanded mass spectrum near to the bare ${\rm C_{60}}^+$ signal, which provides an illustration of some of the more detailed features in the mass spectrum. Apart from ${\rm C_{60}}^+$, the most abundant peaks correspond to ${\rm [C_{60}+(CH_3OH)_m]^+}$ and

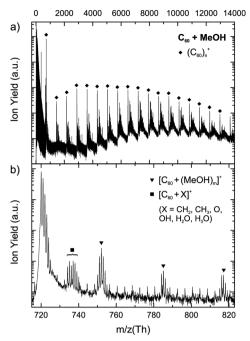


Fig. 1 (a) Positive ion mass spectrum obtained by electron ionization of helium droplets containing both C_{60} and methanol molecules. The pickup pressures were 2.9×10^{-6} mbar and 2.3×10^{-6} mbar, respectively, for the C_{60} and methanol chambers. The oven temperature for evaporation of C_{60} was 371 °C. (b) Expanded view of the region near to the C_{60}^+ peak. As well as the bare C_{60}^+ peaks we also see clear peaks from this ion with up to three methanol molecules attached in this image. Note the pronounced isotope structure derived from the ^{13}C contribution to C_{60} .

 $[C_{60} + (CH_3OH)_mH]^+$ ions. An isotopic analysis shows that the former ions are far more abundant than the latter, with the protonated signal representing 0.2 times of the intensity of the parent for the $[C_{60} + CH_3OH]^+$ complex. This observation is in sharp contrast to the case of pure methanol clusters, where the protonated cluster ion intensity is approximately 30 times that of the corresponding parent ion.²³ Similar values are verified for other cluster sizes. Small fragments derived from methanol, such as CH2, CH3, O and OH, can also be seen attached to the C_{60}^{+} ion. Furthermore, in this particular section of the spectrum there is no evidence for the extensive intra-molecular reactions which result in the loss of multiple dimethyl ether molecules, as was seen in the case of pure methanol clusters. Such reactions would result in $[(CH_3OH)_m(H_2O)_n]$ units attached to the fullerene ions, since the loss of dimethyl ether from methanol clusters yields H₂O. Ions derived from a fullerene cluster with an attached water molecule contribute to the peaks near m/z 740 in Fig. 1(b). However, this most likely derives from pickup of a single water molecule from residual background gas in the pickup chambers, since they are also observed, together with OH and H₃O, in pure C₆₀ experiments with similar ratios.

Fig. 2(a) shows part of the mass spectrum near the $(C_{60})_9^+$ cluster ion, which we can generalize to other $(C_{60})_n^+$ cluster ions. Similar to the spectrum in Fig. 1(b), $(MeOH)_m$ clusters attach to the fullerene cation but here we can see the extent of

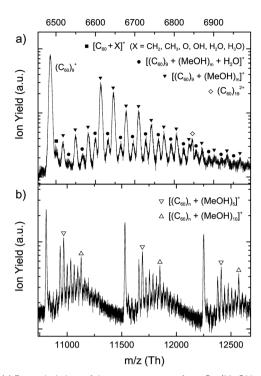


Fig. 2 (a) Expanded view of the mass spectrum for a C_{60}/MeOH mixture in helium nanodroplets near the $(C_{60})_9^+$ peak. In addition to peaks corresponding to $[(C_{60})_9 + (\text{MeOH})_m]^+$ ions, we can also identify peaks from ions where one water molecule is attached to $[(C_{60})_9 + (\text{MeOH})_m]^+$ (circles). Also visible is the doubly ionized $(C_{60})_{19}^{2+}$ ion. (b) Detail in the region of $(C_{60})_{15}^+ - (C_{60})_{17}^+$. The most abundant ions are $(C_{60})_n^+$ ions, followed by mixed clusters containing both C_{60} and methanol molecules. Specially abundant ions containing 5 and 10 methanol units are highlighted.

that process. In this spectrum some strong variations in the abundance of $[(C_{60})_9 + (CH_3OH)_m]^+$ ions are seen. Most strikingly, the signal for $[(C_{60})_9 + (MeOH)_4]^+$ is much stronger than for those ions with fewer methanol molecules, which will be significant in the later discussion. There are also contributions to the mass spectrum from ions of the type $[(C_{60})_n + (MeOH)_m + H_2O]^+$. For pure methanol clusters, successive loss of dimethyl ether was seen producing multiple water molecules within sufficiently large methanol clusters, with a maximum of five attached H2O molecules observed.²³ We see signal from $[(C_{60})_9 + (CH_3OH)_m]^+$ ions with only one H₂O molecule. For pure methanol investigations $[(CH_3OH)_m + H_2O]^+$ ions start to become prominent at m = 7.23According to Fig. 2(a) there are $[(C_{60})_9 + (MeOH)_m + H_2O]^+$ ions starting at m = 1, which indicates that the dehydration reaction took place in a larger cluster, but only part of if reached the detector. No second water molecule was detected for methanol no matter what the cluster size and this, therefore, suggests that the alcohol dehydration reactions suffer strong interference from the presence of the fullerene. Note also that the signals become very weak beyond the attachment of more than 15 MeOH molecules to the fullerene, which contrasts markedly with the large cluster ions seen for pure methanol clusters.²³ It is important to observe that this difference is not related to the signal-to-noise ratio, which was verified to be the same for the measurements of alcohols with and without C₆₀. The apparent difference in this ratio is related to the increased mass/charge range of this work, which is four times the range for pure methanol measurements. Thus, the natural peak broadening effect for high masses becomes more apparent and the baseline goes up, as can be seen in Fig. 1(a).

An illustration of the findings for even larger fullerene cluster ions is shown in Fig. 2(b). Here it becomes apparent that the $[(C_{60})_n + (MeOH)_m]^+$ ion of greatest abundance corresponds to m=5 rather than m=4. In addition, a second prominent peak appears with m=10 after which point the signal declines markedly. Although less easy to see, m=15 is also a magic ion. Doubly ionized, $(C_{60})_n^{2+}$ clusters are also visible in the mass spectrum for odd n=7, albeit literature shows that the smallest doubly charged $(C_{60})_n$ cluster detected corresponds to n=5. $^{32-34}$ Of course, doubly charged clusters with even n might also contribute to the signal of singly charged clusters. However, the abundance of the doubly charged fullerene clusters is small and so will have little effect on our conclusions about singly charged ions.

Ethanol + C₆₀

Fig. 3 shows a section of a mass spectrum obtained by electron ionization of helium droplets doped with C_{60} and ethanol molecules. The overall behavior is broadly similar to that observed in the case of methanol. Magic number ions of the type $[(C_{60})_n + (EtOH)_m]^+$ only become prominent for larger $(C_{60})_n^+$ cluster ions. For even larger $(C_{60})_n^+$ clusters the most prominent ion shifts from m=4 to 5, just as in the methanol case. Also, m=10 is still magic, but not as prominent as in the methanol case.

There is also a change in the chemistry of these ions. Whereas for methanol only cluster ions containing a maximum of one water molecule were observed, a second water molecule can also be seen in the ethanol case. Various fragments attached to the

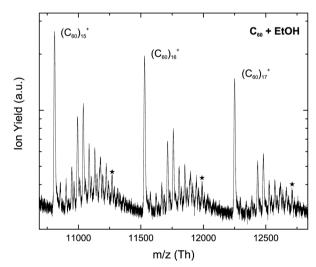


Fig. 3 A section of the mass spectrum measured upon electron ionization of helium droplets doped with C_{60} and ethanol in the region of the $(C_{60})_{16}^+$ cluster. The most pronounced peaks, apart from those from bare $(C_{60})_n^+$ ions, correspond to the attachment of 4 and 5 ethanol molecules to the $(C_{60})_n^+$ cluster. The peaks labelled with an asterisk are for a $(C_{60})_n^+$ ion with 10 attached ethanol molecules.

 $[(C_{60})_n + (EtOH)_m]^+$ were also detected, including C_2H_5 , CHO, CH₂O, CH₃O, CH₄O and CH₅O.

4 Discussion

Paper

We discuss here some of the differences in behavior between the ionization of pure alcohol clusters and the combined C_{60} /alcohol clusters. In doing so we make a number of assumptions. The starting point is that when ionization takes place the positive charge resides on the $(C_{60})_n$ cluster. This is reasonable given that the ionization energy of C_{60} (7.6 eV³⁵) is much lower than that of an alcohol such as methanol (10.85 eV³⁶). The mass spectra essentially confirm this assumption. Specifically, ionization of the alcohol should produce the dominant products seen for the ionization of pure alcohol clusters, namely protonated alcohol clusters. The fact that these are minor products demonstrates that the positive charge quickly finds its way to the fullerene before this particular fragmentation event can take place.

Nevertheless, there is a considerable release of energy as the charge is transferred from He⁺ to the dopants. The ionization energy of atomic helium is 24.59 eV, which means that for a methanol cluster approximately 13.5 eV must be dissipated in some manner by either the dopant cluster and/or helium. When charge transfer occurs from He+ to C60/alcohol clusters there is more than 3.5 eV of additional energy that is released when compared with pure alcohol clusters, and this in itself may account for some of the experimental observations. For example, the observation of much smaller alcohol clusters when the alcohol is combined with C₆₀ might simply be a consequence of evaporative loss of alcohol molecules because of this excess energy release. However, many $(C_{60})_n^+$ ions depart with some alcohol molecules attached and this is presumably because of the favorable binding energy provided by the positive charge on the fullerene cation. In this picture the alcohol molecules furthest away from the fullerene cluster ion are the ones most likely to evaporate and they leave behind a small number of alcohol molecules in contact with the fullerene cation.

It is well known that small alcohol clusters have a tendency to form small rings.^{37,38} The formation of specific sized rings which present an enhanced stability provides a plausible explanation for the pronounced magic number ions observed in the mass spectra. Small $(C_{60})_n^+$ clusters ions with four alcohol molecules show enhanced abundance, whereas for larger ions a switch of the magic numbers to five alcohol molecules is observed. Thus we suggest that four and five-membered ring formation is responsible for these enhanced intensities. The reason for the switch from four-membered to five-membered rings is unclear but may be related to the lower charge density in large $(n \ge 12) (C_{60})_n^+$ cluster ions. The fact that we also see evidence for magic character for attachment of 10 and even 15 alcohol molecules in the case of methanol suggests that multiple rings can form. Note that these could not be linked rings because, in that case, this would not give magic numbers which are simple multiples of 5 alcohol molecules, since some of the molecules will be shared between two rings. Instead,

the conclusion has to be that there are distinct 5-membered rings at different locations across the $(C_{60})_n^+$ cluster ion.

Finally, we note that the sheer increase in surface area for large $(C_{60})_n^+$ cluster ions will assist ring nucleation at different sites. However, an increase in the number of C_{60} molecules brings more than just extra surface area: the number and types of interstitial sites³⁹ between the fullerene molecules also increases. These might work as 'anchor points' about which alcohol rings can form.

5 Conclusions

A mass spectrometric investigation of helium droplets doped with a combination of C₆₀ and a simple alcohol, methanol or ethanol, is reported here. Charged clusters with up to 20 fullerene molecules and 15 alcohol monomers were detected. The results show remarkable differences when compared with the mass spectra of pure alcohol clusters in helium nanodroplets. One major outcome is that clusters are formed with far fewer alcohol molecules than seen for the pure alcohols, an observation which we attribute to evaporative loss of most alcohol molecule after the charge has been transferred to the fullerene. Those alcohol molecules that remain yield magic number ions of the type $[(C_{60})_n + (ROH)_m]^+$ with m = 4 or 5. The m = 4 case is prominent for small n but for larger $(C_{60})_n^+$ clusters the magic numbers switch to m = 5, 10 and 15 for MeOH and to m = 5 and 10 for EtOH. We interpret these findings in term of hydrogenbonded rings formed above the $(C_{60})_n^+$ cluster ions, which yield ions with enhanced stabilities.

Acknowledgements

The work was supported by the FWF (P 26635, P19073 and M 1908-N36). MG acknowledges the Brazilian National Council for the Improvement of Higher Education (CAPES), process no. 4752/11-2. FZ acknowledges the support of the Foundation for Scientific Support of Minas Gerais State (FAPEMIG) and the Brazilian Research Council for Scientific and Technological Development (CNPq).

References

- 1 G. H. Herbig, Astrophys. J., 1975, 196, 129.
- 2 G. H. Herbig, Astrophys. J., 1988, 331, 999.
- 3 H. A. Galue and J. Oomens, Astrophys. J., 2012, 746, 83.
- 4 E. K. Campbell, M. Holz, D. Gerlich and J. P. Maier, *Nature*, 2015, **523**, 322.
- 5 J. P. Maier and E. K. Campbell, *Philos. Trans. R. Soc.*, A, 2016, 374, 20150316.
- 6 G. A. H. Walker, E. K. Campbell, J. P. Maier, D. Bohlender and L. Malo, Astrophys. J., 2016, 831, 130.
- 7 M. Kuhn, M. Renzler, J. Postler, S. Ralser, S. Spieler, M. Simpson, H. Linnartz, A. G. G. M. Tielens, J. Cami, A. Mauracher, Y. Wang, M. Alcamí, F. Martín, M. K. Beyer, R. Wester, A. Lindinger and P. Scheier, *Nat. Commun.*, 2016, 7, 13550.

PCCP

- 8 R. J. Shannon, M. A. Blitz, A. Goddard and D. E. Heard, Nat. Chem., 2013, 5, 745.
- 9 R. Garrod, I. Hee Park, P. Caselli and E. Herbst, Faraday Discuss., 2006, 133, 51.
- 10 S. B. Charnley, M. E. Kress, A. Tielens and T. J. Millar, Astrophys. J., 1995, 448, 232.
- 11 S. Maret, C. Ceccarelli, A. Tielens, E. Caux, B. Lefloch, A. Faure, A. Castets and D. R. Flower, Astron. Astrophys., 2005, 442, 527.
- 12 R. T. Garrod, S. L. W. Weaver and E. Herbst, Astrophys. J., 2008, 682, 283.
- 13 D. C. B. Whittet, A. M. Cook, E. Herbst, J. E. Chiar and S. S. Shenoy, Astrophys. J., 2011, 742, 28.
- 14 E. S. Wirström, W. D. Geppert, A. Hjalmarson, C. M. Persson, J. H. Black, P. Bergman, T. J. Millar, M. Hamberg and E. Vigren, Astron. Astrophys., 2011, 533, A24.
- 15 A. W. Hauser and M. P. de Lara-Castells, Phys. Chem. Chem. Phys., 2017, 19, 1342.
- 16 M. Renzler, M. Daxner, L. Kranabetter, A. Kaiser, A. W. Hauser, W. E. Ernst, A. Lindinger, R. Zillich, P. Scheier and A. M. Ellis, J. Chem. Phys., 2016, 145, 4.
- 17 C. Leidlmair, P. Bartl, H. Schöbel, S. Denifl, M. Probst, P. Scheier and O. Echt, Astrophys. J., Lett., 2011, 738, L4.
- 18 S. Denifl, F. Zappa, I. Mähr, F. F. da Silva, A. Aleem, A. Mauracher, M. Probst, J. Urban, P. Mach, A. Bacher, O. Echt, T. D. Märk and P. Scheier, Angew. Chem., Int. Ed., 2009, 48, 8940.
- 19 S. Denifl, F. Zappa, I. Mähr, A. Mauracher, M. Probst, J. Urban, P. Mach, A. Bacher, D. K. Bohme, O. Echt, T. D. Märk and P. Scheier, J. Chem. Phys., 2010, 132, 234307.
- 20 H. Schöbel, C. Leidlmair, P. Bartl, A. Aleem, M. Hager, O. Echt, T. D. Märk and P. Scheier, Phys. Chem. Chem. Phys., 2011, 13, 1092.
- 21 S. Ralser, A. Kaiser, M. Probst, J. Postler, M. Renzler, D. K. Bohme and P. Scheier, Phys. Chem. Chem. Phys., 2016, 18, 3048.
- 22 S. F. Yang, S. M. Brereton and A. M. Ellis, Int. I. Mass Spectrom., 2006, 253, 79.

- 23 M. Goulart, P. Bartl, A. Mauracher, F. Zappa, A. M. Ellis and P. Scheier, Phys. Chem. Chem. Phys., 2013, 15, 3577.
- 24 K. R. Ryan, L. W. Sieck and J. H. Futrell, J. Chem. Phys., 1964, 41, 111,
- 25 M. S. B. Munson, J. Am. Chem. Soc., 1965, 87, 5313.
- 26 L. W. Sieck, F. P. Abramson and J. H. Futrell, J. Chem. Phys., 1966, 45, 2859.
- 27 R. S. Ruoff, D. S. Tse, R. Malhotra and D. C. Lorents, J. Phys. Chem., 1993, 97, 3379.
- 28 L. F. Gomez, E. Loginov, R. Sliter and A. F. Vilesov, J. Chem. Phys., 2011, 135, 29.
- 29 A. W. Hauser, A. Volk, P. Thaler and W. E. Ernst, Phys. Chem. Chem. Phys., 2015, 17, 10805.
- 30 A. Scheidemann, B. Schilling and J. P. Toennies, J. Phys. Chem., 1993, 97, 2128.
- 31 M. Lewerenz, B. Schilling and J. P. Toennies, J. Chem. Phys., 1995, 102, 8191.
- 32 B. Manil, L. Maunoury, B. A. Huber, J. Jensen, H. T. Schmidt, H. Zettergren, H. Cederquist, S. Tomita and P. Hvelplund, Phys. Rev. Lett., 2003, 91, 215504.
- 33 S. E. Huber, M. Gatchell, H. Zettergren and A. Mauracher, Carbon, 2016, 109, 843.
- 34 A. Mauracher, M. Daxner, S. E. Huber, J. Postler, M. Renzler, S. Denifl, P. Scheier and A. M. Ellis, Angew. Chem., Int. Ed., 2014, 53, 13794.
- 35 D. Muigg, P. Scheier, K. Becker and T. D. Märk, J. Phys. B: At., Mol. Opt. Phys., 1996, 29, 5193.
- 36 W. Tao, R. B. Klemm, F. L. Nesbitt and L. J. Stief, J. Phys. Chem., 1992, 96, 104.
- 37 S. Kasachenco, S. Bulusu and A. J. Thakkar, J. Chem. Phys., 2013, 138, 224303.
- 38 J. F. Garvey, W. J. Herron and G. Vaidyanathan, Chem. Rev., 1994, 94, 1999.
- 39 S. Zöttl, A. Kaiser, P. Bartl, C. Leidlmair, A. Mauracher, M. Probst, S. Denifl, O. Echt and P. Scheier, J. Phys. Chem. Lett., 2012, 3, 2598.